

Performance Evaluation of Big Data Processing Strategies for Neuroimaging

Valérie Hayot-Sasson¹, Shawn T Brown² and Tristan Glatard¹

¹Department of Computer Science and Software Engineering, Concordia University, Montreal, Canada

²Montreal Neurological Institute, McGill University, Montreal, Canada

Abstract—Neuroimaging datasets are rapidly growing in size as a result of advancements in image acquisition methods, open-science and data sharing. However, the adoption of Big Data processing strategies by neuroimaging processing engines remains limited. Here, we evaluate three Big Data processing strategies (in-memory computing, data locality and lazy evaluation) on typical neuroimaging use cases, represented by the BigBrain dataset. We contrast these various strategies using Apache Spark and Nipype as our representative Big Data and neuroimaging processing engines, on Dell EMC’s Top-500 cluster. Big Data thresholds were modeled by comparing the data-write rate of the application to the filesystem bandwidth and number of concurrent processes. This model acknowledges the fact that page caching provided by the Linux kernel is critical to the performance of Big Data applications. Results show that in-memory computing alone speeds-up executions by a factor of up to 1.6, whereas when combined with data locality, this factor reaches 5.3. Lazy evaluation strategies were found to increase the likelihood of cache hits, further improving processing time. Such important speed-up values are likely to be observed on typical image processing operations performed on images of size larger than 75GB. A ballpark speculation from our model showed that in-memory computing alone will not speed-up current functional MRI analyses unless coupled with data locality and processing around 280 subjects concurrently. Furthermore, we observe that emulating in-memory computing using in-memory file systems (tmpfs) does not reach the performance of an in-memory engine, presumably due to swapping to disk and the lack of data cleanup. We conclude that Big Data processing strategies are worth developing for neuroimaging applications.

I. INTRODUCTION

Big Data processing engines have significantly improved the performance of Big Data applications by diminishing the amount of data movement that occurs during the execution of an application. Locality-aware scheduling, introduced by the MapReduce [1] framework, reduced the overall costs associated to network transfer of data by scheduling tasks to the nodes located nearest to the data. Reduction of data movement was further improved upon through in-memory computing [2], which ensures that data is maintained in memory between tasks whenever possible. To further reduce the cost of data movement, lazy evaluation, the process of performing computations only when invoked, was leveraged by Big Data frameworks to enable further optimizations such as regrouping of tasks and computing only what is necessary.

Frameworks such as MapReduce and Spark [2] have become mainstream tools for data analytics, although many others, such as Dask [3], are emerging. Meanwhile, several scientific domains including bioinformatics, physics or astronomy,

have entered the Big Data era due to increasing data volumes and variety. Nevertheless, the adoption of Big Data engines for scientific data analysis remains limited, perhaps due to the widespread availability of scientific processing engines such as Pegasus [4] or Taverna [5], and the adaptations required in Big Data processing engines for scientific computing.

Scientific applications differ from typical Big Data use cases, which might explain the remaining gap between Big Data and scientific engines. While Big Data applications mostly target text processing (e.g. Web search, frequent pattern mining, recommender systems [6]) implemented in consistent software libraries, scientific applications often involve binary data such as images and signals, processed by a sequence of command-line/containerized tools using a mix of programming languages (C, Fortran, Python, shell scripts), referred to as workflows or pipelines. With respect to infrastructure, Big Data applications commonly run on clouds or dedicated commodity clusters with locality-aware file systems such as the Hadoop Distributed File System (HDFS [7]), whereas scientific applications are usually deployed on large, shared clusters where data is transferred between data and compute nodes through shared file systems such as Lustre [8]. Such differences in applications and infrastructure have important consequences. To mention only one, in-memory computing requires instrumentation to be applied to command-line tools.

Technological advances of the past decade, in particular page caching in the Linux kernel [9], in-memory file systems (tmpfs) and memory-mapped files might also explain the lack of adoption of Big Data engines for scientific applications. In such configurations, in-memory computing would be a feature provided by the operating system rather than by the engine itself. The frontier between these two components is blurred and needs to be clarified.

Our primary field of interest, Neuroimaging, is no exception to the generalized rise of data volumes in science due to the joint increase of image resolution and subject cohort sizes [10]. Processing engines have been developed with neuroinformatics applications in mind, for instance Nipype [11] or the Pipeline System for Octave and Matlab (PSOM [12]). Big Data engines have also been used for neuroimaging applications, including the Thunder project [13] and in more specific works such as [14]. However, no quantitative performance evaluation has been conducted on neuroimaging applications to assess the added-value of Big Data engines compared to traditional processing engines.

This paper addresses the following questions:

- 1) What is the effect of in-memory computing, lazy evaluation and data locality on current neuroimaging applications?
- 2) Can in-memory computing be effectively enabled by the operating system rather than the data processing engine?

Answers to these questions have important implications. In [15], a comparative study of Dask, Spark, TensorFlow, MyriaDB, and SciDB on neuroinformatics use-cases is presented. It concludes that these systems need to be extended to better address scientific code integration, data partitioning, data formats and system tuning. We argue that such efforts should only be conducted if substantial performance improvements are expected from in-memory computing, lazy evaluation or data locality. On the other hand, neuroimaging data processing engines are still being developed, and the question remains whether these projects should just be migrated to Spark, Dask, or other Big Data engines.

Our study focuses on performance. We intentionally do not compare Big Data and scientific data processing engines on the grounds of workflow language expressivity, fault-tolerance, provenance capture and representation, portability or reproducibility, which are otherwise critical concerns, addressed for instance in [16]. Besides, our study of performance focuses on the impact of data writes and transfers. It purposely leaves out task scheduling to computing resources, to focus on the understanding of data writes and movement. Task scheduling will be part of our discussion, however.

In terms of infrastructure, we focus on the case of High-Performance Computing (HPC) clusters that are typically available through University facilities or national computing infrastructures such as XSEDE, Compute Canada or PRACE, as neuroscientists typically use such platforms. We assume that HPC systems are multi-tenant, that compute nodes are accessible through a batch scheduler, and that a file system shared among the compute nodes is available. We intentionally did not consider distributed, HDFS-like file systems, as initiatives to deploy them in HPC centers, for instance Hadoop on-demand [17], have not become mainstream yet.

Our methods, including performance models, processing engines, applications and infrastructure used, are described in Section II. Section III presents our results which we discuss in Section IV along with the two research questions mentioned previously. Section V concludes on the relevance of Big Data processing strategies for neuroimaging applications.

II. MATERIALS AND METHODS

The application pipelines, benchmarks, performance data, and analysis scripts used to implement the methods described hereafter are all available at <https://github.com/big-data-lab-team/paper-in-mem-locality> for further inspection and reproducibility. Links to the processing engines and processed data are provided in the text.

A. Engines

1) *Apache Spark*: Apache Spark is a well-established Scala-based processing framework for Big Data, with APIs in Java, Python and R. Its generalized nature allows Spark to

not only be applied to batch workflows, but also SQL queries, iterative machine learning applications, data streaming and graph processing. Spark’s main features include data locality, in-memory processing and lazy evaluation, which it achieves through its principle abstraction, the Resilient Distributed Dataset (RDD).

An RDD is an immutable parallel data structure that achieves fault-tolerance through the concept of lineage [18]. Rather than permitting fine-grained transformations, only coarse-grained transformations (applying to many elements in the RDD), can be applied, thereby making it simple to maintain a log of data modifications. This log, known as the lineage, is used to reproduce any lost data modifications.

Two types of operations can be performed on RDDs: transformations and actions. Applying a transformation to an RDD produces a new child RDD through a narrow or wide dependency. A narrow dependency signifies that the child is only dependent on a single parent partition, whereas a child RDD is dependent on all parent partitions in a wide dependency. Examples of transformations include map, filter and join. To materialize an RDD, an action must be performed, such as a reduce or a collect. Lazy evaluation is represented in Spark through the use of transformations and actions. A series of transformations may be defined without the data ever being materialized. Using this strategy, Spark can optimize data processing throughout the application.

All actions and wide dependencies require a shuffle – Spark’s most costly operation. Every shuffle begins with each map task saving its data to local files for fault tolerance. The shuffle operation then redistributes the data across the partitions as requested. A shuffle marks a stage boundary in Spark, where reduce-like operations will not begin until all dependent map tasks have completed.

Although Spark uses in-memory computing, it is not necessary for all the data to fit in memory. Spark will spill any RDD elements that cannot be maintained in memory to disk. Moreover, as Spark transformations generate new RDDs and numerous transformations may occur within a single application, Spark implements a Least-Recently Used (LRU) eviction policy. If an evicted RDD needs to be reused, Spark will recompute it using the lineage data collected. As demonstrated in [13], caching significantly improves processing times of iterative algorithms where RDDs are reused. It can be of even greater importance if the RDD is costly to recompute.

Data locality in Spark is achieved through the scheduling of tasks to partitions which have the data loaded in memory. If the data is instead stored on HDFS, the scheduler will assign it to one of the preferred locations specified by HDFS. Spark’s scheduler utilizes delay scheduling to optimize fairness and locality for all tasks.

Three different types of schedulers are compatible with Spark: 1) Spark Standalone, 2) YARN [19] and 3) Mesos [20]. The Spark Standalone scheduler is the default scheduler. The YARN scheduler designed for Hadoop [21] clusters and is prepackaged with Hadoop installations, whereas in contrast, Mesos was designed to be used in multi-tenant cluster environments. In our experiments, we focus on the Spark Standalone cluster.

Executing Spark applications on HPC systems with Spark-unaware schedulers may be inefficient. The amount of resources requested by Spark may impede Spark-cluster scheduling time. Using pilot-scheduling strategies to add nodes to the Spark cluster as they are allocated by the underlying schedulers may speedup allocation and overall processing time [22]. This, however, is not studied in the current paper.

As Spark is frequently used by the scientific community, we designed our experiments using the PySpark API. This is at a cost to performance as the PySpark code must undergo Python to Java serialization. We used Spark version 2.3.2 installed from <https://spark.apache.org>.

2) *Nipype*: Nipype is a popular Python neuroimaging processing engine. It aims at being a solution for easily creating reproducible neuroimaging workflows. Although Nipype does not employ any Big Data processing strategies, it provides plugins to numerous schedulers found in most clusters readily available to researchers, such as the Sun/Oracle Grid Engine (SGE/OGE), [TORQUE](#), [Slurm](#) and [HTCondor](#). It also includes its own scheduler, MultiProc, for parallel processing on single nodes. Furthermore, Nipype provides many built-in interfaces to commonly used neuroimaging tools that can be incorporated within the workflows. Nipype’s ability to easily parallelize workflows in researcher-available cluster setups, capture detailed provenance information necessary for reproducibility, and allow users to easily integrate existing neuroimaging tools, make it preferable over existing Big Data solutions, which would necessitate modifications to achieve this.

Jobs, or Interfaces in Nipype, are encapsulated by a Node. A Node dictates that the job will execute on a single input. However, the MapNode, a child variant of the Node, can execute on multiple inputs. All tasks in Nipype execute in their own uniquely named subdirectory which facilitates provenance tracking of inputs and outputs and also enables checkpointing of the workflow. In the case of Node failure or application modification, only the nodes which have been modified (verified by hash) or have not successfully completed, are re-executed.

In order for Nipype to operate as intended, a filesystem shared by all the nodes is required. However, it is still possible to save to a non-shared local filesystem, but it may come at the expense of fault-tolerance, as data located on failed nodes will be permanently lost. Moreover, the user will need to ensure that the files are appropriately directed to the nodes that require them as there is no guarantee of data locality in Nipype.

We used Nipype version 1.1.4 installed through the pip package manager.

B. Data Storage Locations

Data storage location is critical to the performance of Big Data applications on HPC clusters. Data may reside in the engine memory, on a file system whose contents reside in virtual memory (for instance tmpfs), on disks local to the processing node, or on a shared file system. Table I summarizes the Big Data strategies that can be used depending on the data location. In addition, lazy evaluation is available in Spark regardless of data location. The remainder of this

Data Location	In-Memory Computing	Data Locality
In-memory	Yes	Yes
tmpfs	Yes	Yes
Local Disk	Page Caching	Yes
Shared File System	Page Caching	No

TABLE I: Big Data strategies on a shared HPC cluster.

Section explains this Table and provides related performance models.

1) *In-Engine-Memory and In-Memory File System*: The main difference between storing the data in the engine memory, as in Spark, and simply writing to an in-memory file system, such as tmpfs, is what happens when the processed data fills up the available memory. When engine memory is used, the engine must cleanup unused data to avoid crashes. When an in-memory file system is used, the user is responsible ensuring that the filesystem does not reach capacity. Should it be necessary to free up additional memory, the kernel will swap filesystem memory to disk and the performance will become that of local disk writes. In our experiments, we will explore the configuration where the data consumed by the application approaches the threshold of available memory.

2) *Local Disk*: Storing data on local disks inevitably enables data locality, since data transfers are not necessary when tasks are executed on the nodes where the data resides. However, in absence of a more specific filesystem such as HDFS to handle file replication across computing nodes, data locality comes at the price of stringent scheduling restrictions, as tasks can only be scheduled to the single node that contains their input data.

The performance of local disk accesses is strongly dependent on the page caching mechanism provided by the Linux kernel, described in details in [9]. To summarize, data read from disk remains cached in memory until evicted by an LRU (Least Recently Used) strategy. When a process invokes the `read()` system call, the kernel will return the data directly from memory if the requested data lies in the page cache, realizing a cache *hit*. Cache hits drastically speed-up data reads, by masking the disk latency and bandwidth behind a memory buffer. In effect, page caching provides in-memory computing transparently to the processing engine. However, page cache eviction strategies currently cannot be controlled by the application, which prevents processing engines from anticipating reads by preloading the cache. Scheduling strategies might be designed to maximize cache hits, however. For instance, lazy evaluation could result in more cache hits by scheduling data-dependent tasks on the same node.

Page caching has a more dramatic effect on disk writes, reducing their duration by several orders of magnitude. When a process calls the `write()` system call, data is copied to a memory cache that is asynchronously written to disk by flusher threads, when memory shrinks, when “dirty” (unwritten) data grows, or when a process invokes the `sync()` system call. This asynchronous flushing of the page cache is called *write-back*.

Page caching is essentially a way to emulate in-memory computing at the kernel level, without requiring a dedicated engine. The size of the page cache, however, becomes a

limitation when processes write faster than the disk bandwidth. When this happens, the page cache rapidly fills up and writes are limited by the disk write bandwidth as if no page cache was involved.

We introduce the following basic model to describe the filling and flushing of the page cache by an application:

$$d(t) = \left(\frac{D}{C} - \frac{\delta}{\gamma} \right) t + d_0,$$

where:

- $d(t)$ is the amount of data in the page cache at time t
- D is the total amount of data written by the application
- C is the total CPU time of the application
- δ is the disk bandwidth
- γ is the max number of concurrent processes on a node
- d_0 is the amount of data in the page cache at time t_0

This model applies to parallel applications assuming that (1) concurrent processes all write the same amount of data, (2) concurrent processes all consume the same CPU time, (3) data is written uniformly along task execution. With these assumptions, all the processes will write at the same rate, which explains why the model does not depend on the total number of concurrent processes in the application, but only on the max number of concurrent processes executing on the same node (γ). While these assumptions would usually be violated in practice, this simple model already provides interesting insights on the performance of disk writes, as shown later. Naturally, the model also ignores other processes that might be writing to disk concurrently to the application, which we assume negligible here.

In general, an application should ensure that \dot{d} remains negative or null, leading to the following inequality:

$$\frac{D}{C} \leq \frac{\delta}{\gamma} \quad (1)$$

This defines a D/C (data-write) rate beyond which the page cache becomes asymptotically useless. It should be noted that the transient phase during which the page cache fills up might last a significant amount of time, in particular when \dot{d} is positive and small. We intentionally do not model the transient phase as it requires detailed knowledge of difficult to estimate parameters such as the page cache size and the initial amount of data in it (d_0).

We will use Equation 1 to define our benchmarks and interpret the results. It should be noted that leveraging the page cache, and therefore ensuring that Equation 1 holds, has important performance implications: with page caching, the write throughput will be that of memory, while without page caching it will be that of the disk.

3) *Shared File System:* We model a shared file system using its global realized bandwidth Δ , shared by all concurrent processes in the cluster. We are aware that such a simplistic model does not describe at all the intricacies of systems such as Lustre. In particular, metadata management, RPC protocol optimizations and storage optimizations are all covered under the realized bandwidth. We do, however, consider the effect of page caching in shared file systems, since in Linux writes to network-mounted volumes benefit from this feature too.

Data location	Measured write bandwidths (MB/s)
tmpfs	1377.18
Local disk (δ)	193.64
Lustre (Δ)	504.03

TABLE II: Measured bandwidths

As in the local disk model, we note that page caching will only be useful when the flush bandwidth is greater than the write throughput of the application, that is:

$$\frac{D}{C} \leq \frac{\Delta}{\Gamma}, \quad (2)$$

where Γ is the max number of concurrent processes *in the cluster*. Note that $\frac{\Delta}{\Gamma}$ will usually be much lower than $\frac{\delta}{\gamma}$.

C. Infrastructure

All experiments were executed on [Dell EMC's Zenith cluster](#), a Top-500 machine in the [Dell EMC HPC and AI Innovation Lab](#), running Slurm. For the Spark experiments, a Spark cluster was started on a Slurm allocation comprised of 16 dedicated nodes. Each Compute node has Red Hat Enterprise Linux Server release 7.4 (Maipo) as the base operating system with kernel version 3.10.0-693.17.1.el7.x86_64 (patched for Spectre/Meltdown). Dell EMC PowerEdge C6420 with dual Intel Xeon Gold 6148/F processors (40 cores per node) and 192GB (12 × 16 GB), 2666 MHz memory, serve as the compute nodes. Each compute has a 120GB M.2 SATA SSD as local disk. A Dell HPC Lustre Solution with a raw storage of 960TB is accesible on each compute node through a 100 Gb/s Intel OmniPath network. All the nodes connect to a director switch in a 1:1 non-blocking topology. The realized write bandwidth of the local disk, Lustre file system and tmpfs were measured by sequentially writing various numbers of image blocks containing random intensities, to avoid caching effects (see: [measure_bandwidth.py](#)). They are reported in Table II.

D. Datasets

We used BigBrain [23], a 75GB 40 μ m isotropic histological image of a 65-year-old human brain. The BigBrain was selected due to its uniqueness, as there does not yet exist a higher-resolution image of a human brain. Moreover, there currently exists a lack of standardized tools for processing the BigBrain as a consequence of its size. To examine the effects processing the BigBrain has on Big Data strategies, we partitioned the full 3845 × 3015 × 3470 voxel image into 30 (5 × 3 × 2) chunks, 125 (5 × 5 × 5) chunks and 750 (5 × 15 × 10) chunks. Additionally, the full image was also split in half (769 × 603 × 347 voxels) and the half image was partitioned into 125 chunks.

Processing large images is only considered to be part of the Big Data problem in neuroscience. The other problem being the processing large MRI datasets, that is, datasets consisting of many small brain images belonging to various different subjects. This situation is commonly observed in functional MRI (fMRI), where it is becoming increasingly common to process data from hundreds of subjects. Although we have not explored explicitly the processing of large MRI datasets,

the 75GB BigBrain is within the size ballpark [10] of MRI datasets commonly processed in today’s studies.

Since both small and large datasets may need to be processed using the same analysis pipeline, we examined the effects of the data management strategies on small data as well. For this, we selected a 12MB T1W image belonging to subject 1 of OpenNeuro’s ds000001 dataset version 6. In order to split the image into 125 equal-sized chunks, it was necessary to zero-pad the image to the dimensions $165 \times 200 \times 200$ voxels, which subsequently increased the total image size to 13MB.

E. Applications

Algorithm 1 Incrementation

```

1: Input
2:    $x$  a sleep delay in seconds
3:    $n$  a number of iterations
4:    $C$  a set of image chunks
5:    $fs$  filesystem to write to (mem, tmpfs, local disk,
   LUSTRE).
6: for each  $chunk \in C$  do
7:   read  $chunk$  from LUSTRE
8:   for  $i \in [1, n]$  do
9:      $chunk \leftarrow chunk + 1$ 
10:    sleep  $x$ 
11:    if  $i < n$  then
12:      save  $chunk$  to  $fs$ 
13:    end if
14:  end for
15:  save  $chunk$  to LUSTRE
16: end for

```

To effectively investigate how the different strategies impact processing, we selected a simple incrementation pipeline (Algorithm 1) that consists exclusively of map stages. A series of map-only stages would enable us to evaluate the effects of in-memory computing when data locality is preserved. Incrementation was selected over other applications, such as binarization, as it ensured that a new image was created at each step (i.e. no caching effects within the executing application). Each partitioned chunk was incremented by 1, in parallel, by each task. As incrementing images is not a time consuming process, we added a sleep delay to the tasks to study the effects of tasks duration. The incremented chunks would be either maintained in-memory (Spark only) or saved to either tmpfs, local disk or Lustre (Spark and Nipype). Should more than a single iteration be requested, the incremented chunks would be incremented again and saved to the same file system. This would repeat until the number of requested iterations had elapsed. In all conditions, the first input chunks and final output chunks would reside on Lustre. We chose to perform our initial input/final output on Lustre as local storage is typically only accessible to a user for the duration of the execution in HPC environments.

F. Experiments

We conducted four experiments in which we varied (1) the number of iterations in the application (n in Algorithm 1), (2) the task duration (x), (3) the chunk size given a constant image size, (4) the total image size. To evaluate the page-cache model, experiment conditions fell in different regions of Equations 1 and 2, as summarized in Table III. Among the 16 nodes available, 1 was dedicated to the Spark master and driver, and the remaining 15 were used as compute nodes. Since data locality is not normally preserved in Nipype (a new Slurm allocation is requested for each processed task), we instrumented Nipype to ensure data locality (see: [run_benchmarks.py](#)). That is, the chunks were split into partitions, and for each partition, we requested a Slurm allocation to process the entire pipeline in parallel using Nipype’s MultiProc scheduler on a given node. This was possible as no communication was required between the processed chunks.

For our first incrementation experiment, we investigated the effects of Big Data strategies on varying total data size. To achieve this, we increased the number of incrementation iterations from 1, 10 and 100 times. The total data size would then increase from 75GB, at 1 iteration, to 7,500GB, at 100 iterations. The total number of chunks was 125. Chunks all ran concurrently ($\Gamma=125$) and were equally balanced among 15 nodes, leading to 8 or 9 concurrent jobs per node ($\gamma=9$). Task duration was fixed at 3.44 seconds.

In the second experiment, we evaluated the effects of Big Data strategies on varying task duration. If the page cache has sufficient time to flush, it would be expected that in-memory computing and local disk perform equivalently. We varied the task duration between 2.4 and 320 seconds such that the D/C falls into different regions of Equations 1 and 2. The number of chunks was maintained at 125, leading to $\Gamma=125$ and $\gamma=9$. The number of iterations was fixed to 10.

As a third incrementation experiment, we were interested in the effects of chunk size on Big Data strategies. Naturally, a greater chunk size signifies a decrease in parallelism. However, it also signifies an increase in sequential I/O (increased Δ/Γ and δ/γ). For this experiment we partitioned the complete BigBrain image into 30, 125 and 750 chunks, corresponding to γ values of 2, 9 and 25 respectively. While Spark attempted to load-balance the data, it used up only 25 of the 40 cores for 750 chunks. In contrast, Nipype tried to use up as many cores as possible. Unlike the previous experiment, the D/C rate was kept static at 178.6MB/s, however, this ratio ensured that different regions of the inequality were reached depending on amount of parallelism. The number of iterations was fixed to 10, and the task duration was adjusted so that C remained constant at 4,400s.

For our fourth and final incrementation experiment, we investigated the effects of the strategies on different image sizes. We selected the 75GB BigBrain, the 38GB half BigBrain and the 13M T1W MRI image for this experiment. The number of chunks was fixed to 125. Similarly to the previous experiment, the total sequential compute time was fixed (10 iterations, 1.76 seconds per task), however, due to varying size in total data processed (D), the D/C rate varied. Once again,

Experiment 1: Number of Iterations										
n	D (GB)	C (s)	D/C (MB/s)	γ	δ/γ (MB/s)	Γ	Δ/Γ (MB/s)	(D/C)/(δ/γ)	(D/C)/(Δ/Γ)	
1	75	430	178.6	9	21.5	125	4.0	8.3	44.7	
10	750	4,300	178.6	9	21.5	125	4.0	8.3	44.7	
100	7,500	43,000	178.6	9	21.5	125	4.0	8.3	44.7	

Experiment 2: Task Duration										
x (s)	D (GB)	C (s)	D/C (MB/s)	γ	δ/γ (MB/s)	Γ	Δ/Γ (MB/s)	(D/C)/(δ/γ)	(D/C)/(Δ/Γ)	
2.4	750	3,000	256	9	21.5	125	4.0	11.9	64	
3.44	750	4,300	178.6	9	21.5	125	4.0	8.3	44.7	
7.68	750	9,600	80	9	21.5	125	4.0	3.7	20	
320	750	400,000	1.9	9	21.5	125	4.0	0.09	0.48	

Experiment 3: Number of Chunks										
chunks	D (GB)	C (s)	D/C (MB/s)	γ	δ/γ (MB/s)	Γ	Δ/Γ (MB/s)	(D/C)/(δ/γ)	(D/C)/(Δ/Γ)	
30	750	4,400	174.6	2	96.8	30	16.8	1.8	10.4	
125	750	4,400	174.6	9	21.5	125	4.0	8.1	43.7	
750	750	4,400	174.6	25	7.7	375	1.3	22.7	134.3	

Experiment 4: Image Size										
image	D (GB)	C (s)	D/C (MB/s)	γ	δ/γ (MB/s)	Γ	Δ/Γ (MB/s)	(D/C)/(δ/γ)	(D/C)/(Δ/Γ)	
BigBrain	750	2,200	349.1	9	21.5	125	4.0	16.2	87.3	
Half BigBrain	375	2,200	174.6	9	21.5	125	4.0	8.1	43.7	
MRI	0.127	2,200	0.06	9	21.5	125	4.0	0.003	0.015	

TABLE III: Experiment conditions. Red cells denote the conditions where the inequalities in Equations 1 and 2 do not hold, i.e., the page cache is asymptotically useless. Green cells show the conditions where the page cache covers all data writes.

we ensured that the D/C rate fell in multiple different regions of the inequality. The D/C rate ranged from 349.1 MB/s for BigBrain and 174.6MB/s for half BigBrain, to 0.06MB/s for the MRI image. Only the 0.06MB/s MRI satisfied the inequality for both Lustre and local disk.

III. RESULTS

A. Experiment 1: Number of Iterations

Fig. 1a shows the difference between the different filesystem choices given varying number of iterations. At 1 iteration, all filesystems behave the same, although the application was writing faster than the disk bandwidth. This is because application data was not saturating the page cache (transient phase). The page cache, on Zenith, occupies 40% of total memory. With 192 GB of RAM on each node, 76.8 GB of dirty data could be held in a node’s page cache at any given time. As the total amount of data written by the application increases to 750 GB, there is a greater disparity between Lustre and in-memory (2.67 x slower, on average). Local disk performance, however, is still comparable to memory (1.38 x slower, on average). Despite local disk and Lustre both being in transient state, local disk encounters less contention than what would be found on Lustre.

At 100 iterations, or 7,500 GB, Lustre can be found to be, on average, 3.82 x slower than Spark in-memory. The slowdown experienced can be explained by the smaller percentage of total data residing in the page cache at a given time, compared to 10 iterations. Therefore, the effects of Lustre bandwidth are more significant in this application. At 100 iterations, the application was writing 500GB per node (7,500 GB / 15 nodes) and hence could not run on tmpfs or local disk.

While there is some variability that can be seen in Fig. 1a between the two engines, this believed to be insignificant, and potentially due to SLURM node allocation delays in our launching of Nipype.

B. Experiment 2: Task Duration

Increasing task duration ensured that all file systems had a comparable performance (Fig. 1b). Lustre, for instance, is approximately 1.01x slower than Spark in-memory at a task duration of 320 seconds, whereas it is approximately 3.25x slower than Spark in-memory with 2.4 second tasks. This pattern corroborated our page-cache model which postulates that data movement costs will have little impact on compute-intensive tasks. The reasoning behind this is that longer tasks give the page cache more time to flush between disk writes.

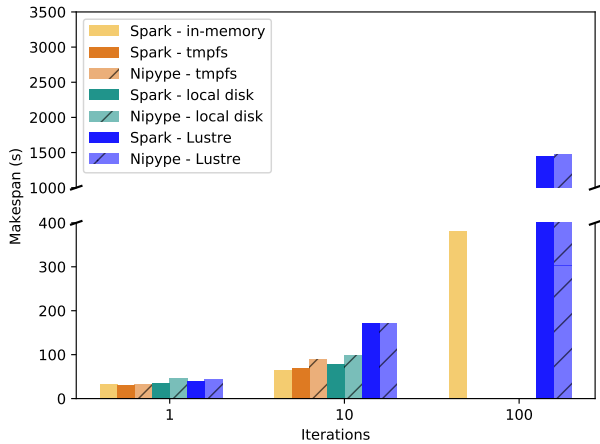
C. Experiment 3: Image Block Size

As can be seen in Fig. 1c, makespan decreases with increasing number of chunks. This is due to the fact that parallelism increases with an increase in number of chunks. At 30 chunks, only 2 CPUs per node are actively working. At 125 chunks, this changes to a maximum of 9 CPUs per node, and at 750 chunks, up to 40 CPUs can be active.

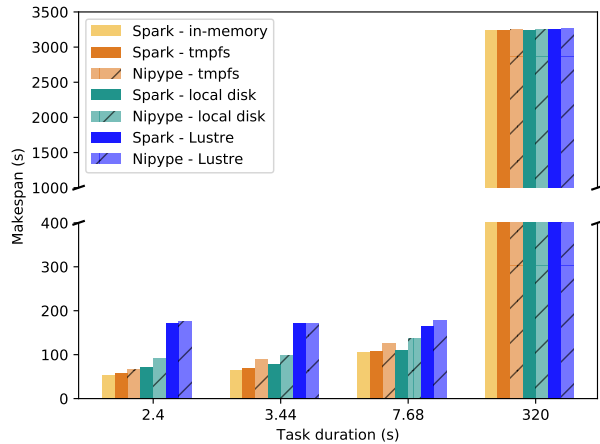
Due to a size limitation of 2 GB imposed on Spark partitions, Spark with in-memory computing processing 30 chunks was not performed.

Local disk and tmpfs perform comparably for all conditions, with Lustre being significantly slower. As with varying the number of iterations, Lustre is slower due to increased filesystem contention, which is, at minimum, 15 x greater than contention on local disk, due to the number of nodes used. With an increase in number of chunks, local disk and tmpfs makespans begin to converge. A potential explanation for this may be that tmpfs is utilizing swap space. As concurrency increases, the memory footprint of the application also increases. It is possible that at 750 chunks, swapping to disk is required by tmpfs, thus resulting in similar processing times as local disk.

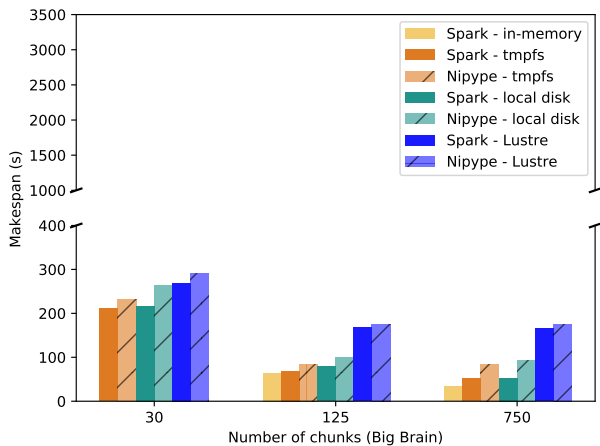
Swapping may also be an explanation for the variance between Spark in-memory and tmpfs performance. While



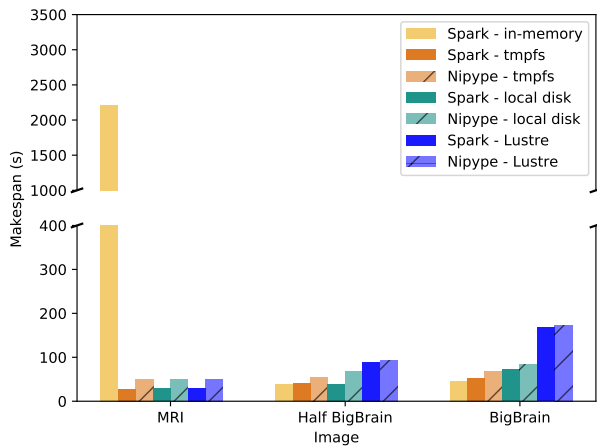
(a) Experiment 1: complete BigBrain, 125 chunks, 3.44-second tasks.



(b) Experiment 2: complete BigBrain, 125 chunks, 10 iterations.



(c) Experiment 3: complete BigBrain, 10 iterations, C= 4,400s.



(d) Experiment 4: 125 chunks, 10 iterations, 1.76-second tasks.

Fig. 1: Experiment results: Makespans of Spark and Nipype writing to memory, tmpfs, local disk and Lustre.

Spark may also spill to disk, it only does so when data does not fit in memory. As none of the RDDs generated throughout the pipeline were cached and all data concurrently accessed could be maintained in-memory, spilling to disk was not necessary.

D. Experiment 4: Image Size

Increasing overall data size decreases performance, as can be seen in Fig. 1d. When the data size is very small (e.g. MRI image) all file system makespans are comparable. This is due to the fact that page cache can be leveraged fully regardless of file system. However, this time, Spark in-memory performed significantly worse than all other filesystems, with a makespan of 2,211 seconds. Upon further inspection, it appeared that Spark in-memory executed in a sequential order, on a single worker node. Lack of parallelism for the MRI image may be a result of Spark’s maximum partition size, which is by default 128 MB – significantly larger than the 13 MB MRI image.

At half BigBrain, the makespan differences become apparent in both local disk and Lustre, with Lustre becoming 2.4x slower than in-memory. This can be attributed to page cache saturation, as predicted by the model for both half the BigBrain

image and the complete BigBrain. Only the MRI image was predicted to fall within the model constraints.

When the complete BigBrain is processed, the disparity between the different filesystems becomes even greater. Lustre becomes 3.68x slower, whereas local disk becomes 1.68x slower. An explanation for this is that the page cache fills up faster due to data size.

E. Page Cache Model Evaluations

In order to evaluate the page cache model, we compared the observed speedup ratio provided by in-memory computing to the $(D/C) / (\delta/\gamma)$ and $(D/C) / (\Delta/\Gamma)$ ratios (Fig. 2). Speed-up ratios were computed as the ratio between the makespan obtained with Spark on local disk or Lustre, and the makespan obtained with Spark for in-memory computing. Experiments for which there were no in-memory equivalent (i.e. BigBrain split into 30 chunks) were not considered.

Results show that, overall, the model correctly predicted the effect of page cache on processing times for local disk and Lustre. That is, the speed-up provided by in-memory computing was larger than 1 for D/C rates larger than δ/γ (local disk)

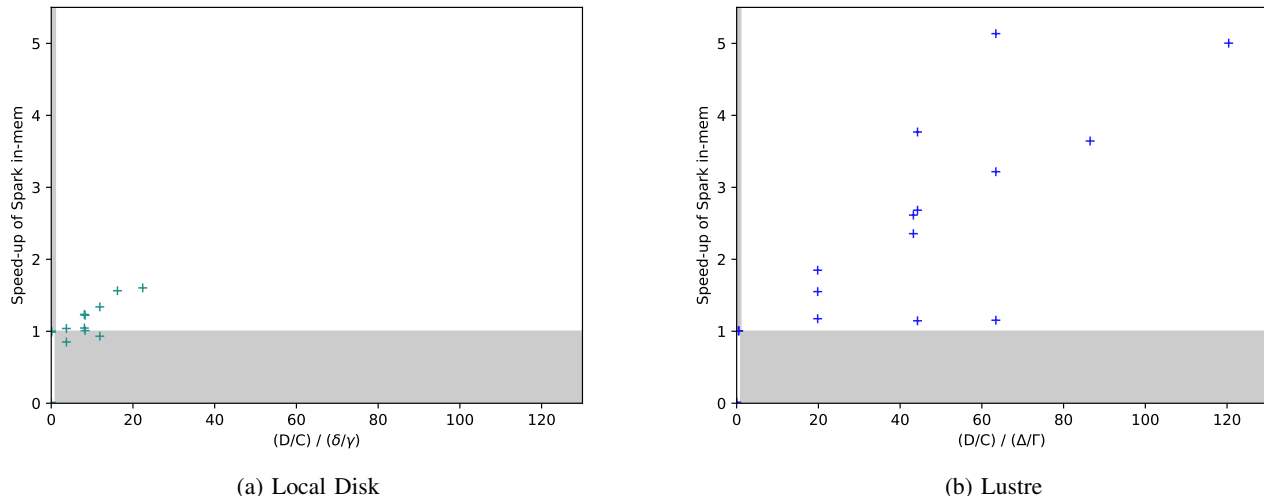


Fig. 2: Page cache model evaluation. Grey regions denote areas that violate model predictions.

or Δ/Γ (Lustre). Conversely, the speed-up provided by in-memory computing remained close to 1 for D/C rates smaller than δ/γ (local disk) or Δ/Γ (Lustre). The two points close to the origin correspond to the sequential processing of the MRI image by Spark mentioned previously.

Points which violated model predictions were found at 1 iteration, where page cache would not have been saturated in spite of a high D/C (transient state). However, in all cases, the “1” boundary was never trespassed by more than a factor of 0.19, and is therefore likely a result of system variability.

IV. DISCUSSION

A. Effect of In-Memory Computing

We measured the effect of in-memory computing by comparing the runs of Spark in-memory (yellow bars in Fig. 1) to the ones of Spark on local disk (non-hatched green bars). The speed-up provided by in-memory computing is also reported in Fig. 2a. The speed-up provided by in-memory computing increases with $(D/C) / (\delta/\gamma)$, as expected from the model. In our experiments, it peaked at 1.6, for a ratio of 16.2. This correspond to the processing of the BigBrain with 125 chunks and 1.76-second tasks in experiment 4 (total computing time $C=2,200s$), which is typically encountered in common image processing tasks such as denoising, intensity normalization, etc. The speed up of 1.6 is also reached with a ratio of 22.7 in experiment 3, obtained by processing the BigBrain with 750 chunks.

The results also allow us to speculate on the effect of in-memory computing on the pre-processing of functional MRI, another typical use case in neuroimaging. Assuming an average processing time of 20 minutes per subject, which is a ballpark value commonly observed with the popular [SPM](#) or [FSL](#) packages, an input data size of 100MB per subject, and an output data size of 2GB (20-fold increase compared to input size), the D/C rate would be 1.8MB/s, which would reach the δ/γ threshold measured on this cluster for $\gamma = 108$, that is, if 108 subjects were processed on the same node. This

is very unlikely as the number of CPUs per node was 40. We therefore conclude that in-memory computing is likely to be useless for fMRI analysis. Naturally, this estimate is strongly dependent on the characteristics of the cluster.

B. Effect of Data Locality

We measure the effect of data locality by comparing the runs of Spark on local disk (non-hatched green bars in Fig. 1) to the ones of Spark on Lustre (non-hatched blue bars). The speed-up provided by local execution peaked at 3.2, for 750 chunks in experiment 3. Overall, writing locally was usually preferable over writing to Lustre, as a result of the lower contention on local disk. Although it may be true that network bandwidths exceed that of disks [24], locality remains important as contention on a shared filesystem tends to be much higher than on local disk. The only time writing locally did not have significant impact over Lustre was in experiments 1 and 4, at 1 iteration and when processing the MRI image, respectively. In both these scenarios, the Lustre writes did not impact performance as the data was able to be written to page cache and flushed to Lustre asynchronously.

C. Combined Effect of In-Memory and Data Locality

We measure the combined effect of data locality and in-memory computing by comparing the runs of Spark in-memory (yellow bars in Fig. 1) to the ones of Spark on Lustre (non-hatched blue bars). The speed-up provided by the combined use of data locality and in-memory computing is also reported in Fig. 2b. The provided speed-up increases with $(D/C) / (\Delta/\Gamma)$, as expected from the model. In our experiments, it peaked around 5, for ratios of 120.4 and 64. Again, this configuration is likely to happen in typical image processing tasks performed on the BigBrain.

As for the fMRI speculation, the D/C rate of 1.8MB/s would reach the Δ/Γ threshold for $\Gamma = 280$, which is a realistic number of subjects to process on a complete cluster. Naturally, this estimate is highly dependent on the observed bandwidth of the shared file system (Δ).

D. Effect of Lazy Evaluation

The effects of lazy evaluation can be seen throughout the experiments. Nipype was found to be slower than Spark in most experiments. While the Nipype execution graph is generated prior to workflow execution, there are no optimizations to ensure that the least amount of work is performed to produce the required results.

During the processing of Experiment 3, 750 chunks were processed in two batches for both Spark and Nipype due to CPU limitations. Rather than running each iteration on the full dataset, as with Nipype, Spark opted to perform all the iterations on the first batch (load, increment, save), and then proceeded to process the second batch. Such an optimization is important, even when processing data on disk, as it would presumably increase the occurrence of cache hits. This may partially explain the speedup seen at 750 chunks in Figure 1c.

E. Can tmpfs and Page Caches Emulate In-Memory Computing?

Although tmpfs and page cache do improve performance, as seen in Figure 1, they do not always perform equivalently to in-memory. Tmpfs's main limitation is that data residing on it may be swapped to disk if the system's memory usage is high. When it reaches this point, its performance slows down to swap disk bandwidth, as observed in Figure 1d. Page cache suffers a similar dilemma. I/O blocking writes to disk occur when a given percentage (e.g. 40 %) of total memory is occupied by dirty data. When the threshold is exceeded, processes performing writes must wait for dirty data to be flushed to disk.

Furthermore, like memory, tmpfs and page cache are shared resources on a node. If users on the node are heavily using memory to incite tmpfs to writes to swap space, or are performing data-intensive operations that fill up the page cache, tmpfs/page cache performance on will be limited for other users. However, it is possible to request through the HPC scheduler a certain amount of available memory. Ultimately, in-memory data will also need to be spilled to disk if memory usage exceeds amount of available memory, although disk writes are likely to occur in tmpfs and page cache before requested available memory is filled.

F. Scheduling Remarks

A common recommendation in Spark is to limit the number of cores per executors to 5, to preserve a good I/O throughput (see [Cloudera blog](#)), but the rationale for this recommendation is hardly explained. We believe that throughput degradation observed with more than 5 cores per executor might be coming from full page caches.

Spark does not currently include any active management of disk I/Os or page caches. We believe that it would be beneficial to extend it toward this direction, to increase the performance of operations where local storage has to be used, such as disk spills or shuffles. For instance, workflow-aware cache eviction policies that maximizes page cache usage for the workflows could be investigated.

An alternative Nipype plugin designed for running on Slurm was not used in the experiments. The Slurm plugin requests a Slurm allocation for each processed data chunk. Such a scheduling strategy was not ideal in our environment where oversubscription of nodes was not enabled.

Unlike Spark, Nipype by default opts to use all available CPUs rather than to load balance data across the cluster. That is, given 50 chunks and 40 cores, Spark will only use up 25 cores and process in two batches. Nipype will also have no choice but to split up the processing into two batches, but will first process 40 chunks, immediately followed by the remaining 10. While both are reasonable strategies for data processing, Spark may end up benefiting more from the page cache, as less data is written in parallel (25 vs 40), giving more time for the page cache to flush.

Nipype's MapNodes, which apply a given function to each element in a list, were found to be slower than the Node, which apply a function to a single element, due to a blocking mechanism. For this reason, we selected to iterate through a series of Nodes in our code despite MapNodes being easier to use.

G. Other Comments

Writing to node-local storage in a cluster environment comes at a cost, for both Nipype and Spark without HDFS. When a node is lost, the node-local data is lost with it. While Spark will recompute the lost partition automatically using lineage, Nipype will fail for all tasks requiring the data. Nevertheless, Spark will also fail if RDDs of node-local filenames are shuffled, as the data associated to the filenames will not be shuffled with the RDD and there will be no mechanism in place to fetch it.

When executed on Lustre, Nipype will checkpoint itself, ensuring resumption from last checkpoint during re-execution. This is particularly important in the case of compute-intensive applications, such as those found in neuroimaging. Spark also provides a checkpointing mechanism, however, it requires HDFS.

It is common in neuroimaging applications for users to want access to all intermediate data. Such a feature is currently only possible when writing to shared filesystem. It would also not be an option with Spark in-memory. To enable this, burst buffers or heterogeneous storage managers (e.g. Triple-H [25]) could be used to ensure fast processing and that all outputs (including intermediate outputs) will be sent asynchronously to the shared filesystem.

It was expected that Spark would experience longer processing times, particularly with the small datasets, due to Java serialization. This was not found to be the case. Unlike Spark, Nipype performs a more thorough provenance capture, potentially owing to longer processing times.

In this paper, we analyzed the effects of Big Data strategies on an map-only artificial neuroimaging pipeline. This allowed us to examine the effects of these strategies without being significantly obscured by other conditions. Studying the effects of such strategies on map-reduce type workflows, in addition to real neuroimaging pipelines, would allow us to gain further

insight on the added value of the Big Data performance strategies for neuroimaging use cases remains to be done.

V. CONCLUSION

Big Data performance optimization strategies help improve performance of typical neuroimaging applications. Our experiments indicate that overall, in-memory computing enables greater speedups than what can be obtained by using page cache and tmpfs. While page cache and tmpfs do give memory-like performance, they are likely to fill up faster than memory, leading to increased performance penalties when compared to in-memory computing. We conclude that extending Big Data processing engines to better support neuroimaging applications, including developing their provenance, fault-tolerance, and reproducibility features, is worthwhile.

Data locality plays an important role in application performance. Local disk was found to perform better than the shared filesystem despite having lower bandwidth, due to increased contention on the shared filesystem. Since local disk typically has less contention than shared filesystems, it is recommended to store data locally. However, using local storage without a distributed file system may limit fault tolerance.

Although a more thorough analysis of lazy evaluation remains to be performed, it is speculated that this may be the cause of the general performance difference between Spark and Nipype. Furthermore, it was found that lazy evaluation optimizations increase the likelihood of cache hits, thus improving overall performance.

Even though Big Data strategies are beneficial to the processing of large images, it is estimated that it would require running a functional MRI dataset with 280 concurrent subjects for any noticeable impact using our Lustre bandwidth estimate. Benchmarking Spark and Nipype using such a large fMRI dataset would be a relevant follow-up experiment, to test this hypothesis. It would also be useful to evaluate other types of applications, such as ones containing data shuffling steps.

Finally, we plan to extend this study by including task scheduling strategies in a multi-tenant environment. We expect to observe important differences between Spark and Nipype, due to Spark's use of overlay scheduling. The impact of other Big Data technologies, such as distributed in-memory file systems (e.g. [Apache Ignite](#)) and Lustre scalability issues [26], could also be investigated.

VI. ACKNOWLEDGMENTS

We are thankful to the Dell EMC HPC and AI Innovation Lab in Roundrock, TX, for providing the infrastructure and high-quality technical support.

REFERENCES

- [1] J. Dean and S. Ghemawat, "MapReduce: simplified data processing on large clusters," *Comm. of the ACM*, vol. 51, no. 1, pp. 107–113, 2008.
- [2] M. Zaharia, R. S. Xin, P. Wendell, T. Das, M. Armbrust, A. Dave, X. Meng, J. Rosen, S. Venkataraman, M. J. Franklin, *et al.*, "Apache Spark: a unified engine for big data processing," *Comm. of the ACM*, vol. 59, no. 11, pp. 56–65, 2016.
- [3] M. Rocklin, "Dask: Parallel computation with blocked algorithms and task scheduling," in *Proc. of the 14th Python in Science Conference*, no. 130-136. Citeseer, 2015.
- [4] E. Deelman, G. Singh, M.-H. Su, J. Blythe, Y. Gil, C. Kesselman, G. Mehta, K. Vahi, G. B. Berriman, J. Good, *et al.*, "Pegasus: A framework for mapping complex scientific workflows onto distributed systems," *Scientific Programming*, vol. 13, no. 3, pp. 219–237, 2005.
- [5] T. Oinn, M. Addis, J. Ferris, D. Marvin, M. Senger, M. Greenwood, T. Carver, K. Glover, M. R. Pocock, A. Wipat, *et al.*, "Taverna: a tool for the composition and enactment of bioinformatics workflows," *Bioinformatics*, vol. 20, no. 17, pp. 3045–3054, 2004.
- [6] J. Leskovec, A. Rajaraman, and J. D. Ullman, *Mining of massive datasets*. Cambridge university press, 2014.
- [7] K. Shvachko, H. Kuang, S. Radia, and R. Chansler, "The Hadoop distributed file system," in *Mass storage systems and technologies (MSST), 2010 IEEE 26th symposium on*. Ieee, 2010, pp. 1–10.
- [8] P. Schwan *et al.*, "Lustre: Building a file system for 1000-node clusters," in *Proc. of the 2003 Linux symposium*, 2003, pp. 380–386.
- [9] R. Love, *Linux kernel development*. Pearson Education, 2010.
- [10] J. D. Van Horn and A. W. Toga, "Human neuroimaging as a Big Data science," *Brain imaging and behavior*, vol. 8, no. 2, pp. 323–331, 2014.
- [11] K. Gorgolewski, C. D. Burns, C. Madison, D. Clark, Y. O. Halchenko, M. L. Waskom, and S. S. Ghosh, "Nipype: a flexible, lightweight and extensible neuroimaging data processing framework in Python," *Frontiers in neuroinformatics*, vol. 5, p. 13, 2011.
- [12] P. Bellec, S. Lavoie-Courchesne, P. Dickinson, J. Lerch, A. Zijdenbos, and A. C. Evans, "The pipeline system for Octave and Matlab (PSOM): a lightweight scripting framework and execution engine for scientific workflows," *Frontiers in neuroinformatics*, vol. 6, p. 7, 2012.
- [13] J. Freeman, N. Vladimirov, T. Kawashima, Y. Mu, N. J. Sofroniew, D. V. Bennett, J. Rosen, C.-T. Yang, L. L. Looger, and M. B. Ahrens, "Mapping brain activity at scale with cluster computing," *Nature methods*, vol. 11, no. 9, p. 941, 2014.
- [14] M. Makkie, H. Huang, Y. Zhao, A. V. Vasilakos, and T. Liu, "Fast and scalable distributed deep convolutional autoencoder for fMRI Big Data analytics," *Neurocomputing*, vol. 325, pp. 20–30, 2019.
- [15] P. Mehta, S. Dorkenwald, D. Zhao, T. Kaftan, A. Cheung, M. Balazinska, A. Rokem, A. Connolly, J. Vanderplas, and Y. AlSaiyad, "Comparative evaluation of Big-Data systems on scientific image analytics workloads," *Proc. of the VLDB Endowment*, vol. 10, no. 11, pp. 1226–1237, 2017.
- [16] T. Guedes, V. Silva, M. Mattoso, M. V. N. Bedo, and D. de Oliveira, "A practical roadmap for provenance capture and data analysis in spark-based scientific workflows," in *Workshop on Workflows in Support of Large-Scale Science (WORKS)*, Dallas, TX, 2018.
- [17] S. Krishnan, M. Tatineni, and C. Baru, "myHadoop-Hadoop-on-Demand on traditional HPC resources," *San Diego Supercomputer Center Technical Report TR-2011-2*, University of California, San Diego, 2011.
- [18] M. Zaharia, M. Chowdhury, M. J. Franklin, S. Shenker, and I. Stoica, "Spark: Cluster computing with working sets." *HotCloud*, vol. 10, no. 10-10, p. 95, 2010.
- [19] V. K. Vavilapalli, A. C. Murthy, C. Douglas, S. Agarwal, M. Konar, R. Evans, T. Graves, J. Lowe, H. Shah, S. Seth, *et al.*, "Apache Hadoop YARN: Yet another resource negotiator," in *Proc. of the 4th annual Symposium on Cloud Computing*. ACM, 2013, p. 5.
- [20] B. Hindman, A. Konwinski, M. Zaharia, A. Ghodsi, A. D. Joseph, R. H. Katz, S. Shenker, and I. Stoica, "Mesos: A platform for fine-grained resource sharing in the data center," in *NSDI*, vol. 11, no. 2011, 2011, pp. 22–22.
- [21] T. White, *Hadoop: The definitive guide*. O'Reilly Media, Inc., 2012.
- [22] I. Paraskevagos, A. Luckow, G. Chantzialexiou, M. Khoshlessan, O. Beckstein, G. C. Fox, and S. Jha, "Task-parallel analysis of molecular dynamics trajectories," *CoRR*, vol. abs/1801.07630, 2018.
- [23] K. Amunts, C. Lepage, L. Borgeat, H. Mohlberg, T. Dickscheid, M.-É. Rousseau, S. Bludau, P.-L. Bazin, L. B. Lewis, A.-M. Oros-Peusquens, *et al.*, "BigBrain: an ultrahigh-resolution 3D human brain model," *Science*, vol. 340, no. 6139, pp. 1472–1475, 2013.
- [24] G. Ananthanarayanan, A. Ghodsi, S. Shenker, and I. Stoica, "Disk-locality in datacenter computing considered irrelevant," in *HotOS*, vol. 13, 2011, pp. 12–12.
- [25] N. S. Islam, X. Lu, M. Wasi-ur Rahman, D. Shankar, and D. K. Panda, "Triple-h: A hybrid approach to accelerate hdfs on hpc clusters with heterogeneous storage architecture," in *Cluster, Cloud and Grid Computing (CCGrid), 2015 15th IEEE/ACM International Symposium on*. IEEE, 2015, pp. 101–110.
- [26] N. Chaimov, A. Malony, S. Canon, C. Iancu, K. Z. Ibrahim, and J. Srinivasan, "Scaling spark on hpc systems," in *Proc. of the 25th ACM International Symposium on High-Performance Parallel and Distributed Computing*. ACM, 2016, pp. 97–110.